Harmonic Generation from Neutral Manganese Atoms in the Vicinity of the Giant Autoionization Resonance

M. A. Fareed,[1] V. V. Strelkov,[2,3] M. Singh,[1] N. Thiré,[1] S. Mondal,[1,4] B. E. Schmidt,[1,5] F. Légaré,[1] and T. Ozaki[1,*]

[1]*Institut National de la Recherche Scientifique—Centre Energie Matériaux Télécommunications, 1650 Lionel-Boulet, Varennes, Québec J3X 1S2, Canada*

[2]*A. M. Prokhorov General Physics Institute of RAS, Vavilova Street 38, 119991 Moscow, Russia*

[3]*Moscow Institute of Physics and Technology (State University), 141700 Dolgoprudny, Moscow Region, Russia*

[4]*ELI-ALPS, ELI-Hu Kft., Dugonics ter 13, H-6720 Szeged, Hungary*

[5]*few-cycle, Inc., 2890 Rue de Beaurivage, Montreal, Quebec H1L 5W5, Canada*

High harmonics from laser-ablated plumes are mostly generated from ionic species. We demonstrate that with ultrashort infrared (∼1.82 μm) driving lasers, high harmonics from laser-ablated manganese are predominantly generated from neutral atoms, a transition metal atom with an ionization potential of 7.4 eV. Our results open the possibility to advance laser-ablation technique to study the dynamics of neutral atoms of low ionization potential. Moreover, as manganese contains giant autoionizing resonance, intense and broadband high harmonics have been demonstrated from this resonance at energies from 49 to 53 eV. This opens the possibility to generate intense attosecond pulses directly from the giant resonances, as well as to study these resonances using high-harmonic spectroscopy.

High harmonics are an attractive method to produce coherent extreme ultraviolet (XUV) and soft x-ray radiation [1,2]. These radiation sources are essential tools to study attosecond science [3], ultrafast XUV spectroscopy [4], molecular tomography [5], and imaging [6]. Moreover, high-harmonic spectroscopy (HHS) is an attractive technique to study electron dynamics at its natural timescale. A few examples of HHS studies are electron-ion recollisions, multielectron interaction [7], photoionization cross-section (PICS) measurement [8], and charge migration [9].

Over the last three decades, high harmonics have been demonstrated from atoms, molecules, and solids [10]. The atomic and molecular species can be produced either by using gas jets [1,2,11] or by laser ablation [12,13]. The high-harmonic generation (HHG) process from atoms and small molecules is explained by the semiclassical three-step model [14] for gas jets and most laser-ablated plumes (LAPs). According to this model, when ultrafast radiation interacts with an atom or molecule, an electron is tunnel ionized from the ground state, accelerates in the continuum and, finally, photorecombines to the ground state. The high-harmonic cutoff is estimated with the three-step model $E_{\text{cutoff}}[\text{eV}] = I_p + 3.17U_p = I_p + 2.96 \times 10^{-13}I[\text{W/cm}^2](\lambda[\mu\text{m}])^2$, where I_p, U_p, I, and λ are the ionization potential, ponderomotive energy, laser intensity, and wavelength, respectively. In a medium with sufficient density, this process occurs in a large number of particles and the phase matched coherent buildup of emitted photons produces the XUV to soft x-ray pulse [3].

In HHG from LAPs, the nonlinear media is produced from a solid target [12]. As such, it has the advantage of being able to generate high harmonics from any material in solid form, thus drastically widening the choice of atoms and molecules for studying their ultrafast and attosecond dynamics through HHS. Moreover, many laser-ablated media used for HHG contain different resonances [15,16], such as autoionizing resonance, giant autoionizing resonance (GAR), etc. It is observed that these resonances change the characteristics of the high-harmonic spectra in the vicinity of the resonance involved. Therefore, HHG from LAPs also allows one to study the dynamics of such resonances via HHS at unprecedented time resolution. The contribution of narrow-bandwidth autoionizing resonances in HHG has been extensively studied [15,17–19], and the four-step model explains the HHG process from these resonances [20,21]. However, the role of GAR in HHG is not clear due to the lack of experimental evidence, as discussed later in the introduction. Moreover, it has been reported that harmonics from LAPs using near-infrared driving fields are mostly generated from ionic species of high ionization energies (e.g., $I_{p_{\text{Mn}^+}} = 15.64$ eV, $I_{p_{\text{Mn}^{2+}}} = 33.63$ eV) [22]. Neutral atoms having low ionization potentials (e.g., $I_{p_{\text{Mn}}} = 7.4$ eV) do not generate high harmonics efficiently (in spite of the high ionization probability) because of the low saturation intensity leading to low cutoff (for neutral manganese; $I_{\text{sat}} < 0.5 \times 10^{14}$ W/cm² and $E_{\text{cutoff}} < 17$ eV for a 0.8 μm wavelength). Although harmonics from ions have the advantage

of a large cutoff, one of its disadvantages was that we were not able to study the ultrafast dynamics of materials in their neutral phase, such as for free neutral atoms or those bound in a molecule or solid.

There is growing interests from the scientific community to study the impact of GAR on the ultrafast ionization dynamics of transition metal atoms [23,24]. HHS is useful to study the dynamics of such resonances at unprecedented times. As such, it is of considerable importance to find conditions for HHG from neutral transition metal atoms and study the ionization and emission dynamics of their GAR at attosecond timescales. Moreover, GAR are broadband in nature, which can be used for multiple studies, such as the generation of intense and broadband high harmonics, the study of their multielectron dynamics, estimates of the PICS [7,8,25,26], and understanding of the ultrafast dynamics in the solid phase [27]. Therefore, studying the ultrafast dynamics of GAR could reveal new and important phenomena that are rich in physics. Moreover, the exact role of multielectrons in HHG is not clear. To date, only a few studies have been done to understand the role of giant resonance in HHG. For example, in 2011, Shiner et al. demonstrated intense harmonics from a giant resonance of xenon of around 100 eV [8], which was earlier predicted by Frolov et al. [7]. Shiner et al. used a distinguishable-electron picture to explain HHG from the giant resonance and proposed that the peak at 100 eV is observable due to the strong Coulomb interaction between the continuum electron (tunnel ionized from the $5p$ state) and inner-shell $4d$ electron [lying in the orbital ($m = 0$)]. Later, Pabst and Santra [28] showed theoretically that, in xenon, all electrons from the $4d$ orbitals ($m = 0, \pm1, \pm2$) contribute to broadband HHG. Recently, Faccialà et al. [29] studied the dynamics of xenon harmonics with two-color multicycle fields and demonstrated how this control scheme can be used to investigate the role of electron correlations that give birth to the giant resonance.

Studying the GAR of neutral manganese atoms using HHS would be important for understanding the involvement of GAR in HHG since they are simpler in nature than that of xenon [23,30]. For example, the $3p$-$3d$ resonance of neutral manganese involves a $3p$-$3d$ channel and lies below the $3p$ ionization threshold—unlike the dominant $4d$-$5f$ continuum GAR of xenon, which involves multiple channels and is located above the $4d$ ionization threshold.

In this Letter, we study high harmonics from laser-ablated manganese using 1.82 μm infrared (IR) fields with various pulse durations. We find that high harmonics are generated from neutral manganese, which has a low ionization potential of 7.4 eV. Moreover, manganese contains GAR at energies of around 50 eV. Intense and broadband high harmonics from the GAR are demonstrated at energies ranging from 49 to 53 eV. The high energy region of XUV from neutral manganese is achieved by using ultrashort pulses ($\sim$12 fs). Our observation of high harmonics from neutral manganese opens a perspective to advance the laser-ablation technique for the ultrafast and attosecond study of neutral atoms. Furthermore, the low ionization potential of such elements will be useful for essentially reducing the laser intensity, and thus relaxing requirements for the laser setup for HHG. This higher accessibility could lead to an even wider application of high harmonics from LAP. Furthermore, high harmonics from GAR opens the possibility to use these resonances for intense attosecond pulse generation and study their multielectron dynamics at attosecond timescales.

The schematic diagram of the experimental setup used for HHG is shown in Fig. 1. Complete details of the $\sim$1.82 μm wavelength IR laser used for HHG can be found elsewhere [31,32]. In short, high harmonics are generated from manganese plumes using IR fields with various pulse durations. First, an IR laser pulse with $\sim$1 mJ energy and $\sim$50 fs pulse duration was generated using an optical parametric amplifier (HE-TOPAS). These IR pulses were amplified to 10 mJ in a type-II β barium borate crystal. The pulse duration of these pulses was 50 fs. In the first step, these pulses were directly used for HHG. After that, amplified IR pulses were then focused onto a 3-m-long hollow-core fiber for spectral broadening, then compressed up to few-cycle duration using a 3-mm-thick fused silica plate. Finally, these pulses, with pulse durations of 30 and 12 fs, were focused onto the manganese plume with a diameter of 140 μm for HHG. For the plume ablation, laser pulses with a pulse duration of $\sim$210 ps and a laser intensity of $\sim$10^{10} W/cm^2 were focused earlier ($\sim$45 ns) on solid manganese over a diameter of 200 μm that can produce a plume with a length of $\sim$1 mm [13]. The density of this LAP is estimated to be $\sim$10^{17} cm^{-3} [16]. Finally, the high-harmonic spectra were recorded using an imaging spectrometer composed of an XUV grating (1200 lines/mm; Hitachi), a microchannel plate (MCP), and a CCD camera.

Neutral manganese has an ionization potential of 7.4 eV and it contains GAR of around 50 eV [33]. The role of neutral manganese and its GAR in HHG is investigated with an IR field at pulse durations from 50 to 12 fs. Figure 2(a) shows the high-harmonic spectra recorded using 50 (black spectra) and 30 fs (blue spectra) pulses. With a 50 fs laser, despite the relatively higher intensity, high harmonics up to 36 eV are observed. Note that this cutoff is also observed at a lower laser intensity of $\sim$1 × 10^{14} W/cm^2. From the high-harmonic cutoff, we
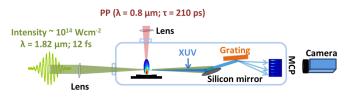

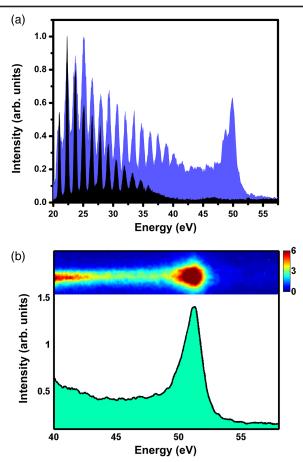FIG. 1. Schematic diagram of the experimental setup used for high-harmonic generation.

(a)

(b)

FIG. 2. (a) Harmonic spectra observed from manganese plumes with pulse durations of ∼30 (blue spectra) and 50 fs (black spectra), wavelength of 1.82 μm, and laser intensities of ∼4.0 × 10^14 W/cm² and ∼5 × 10^14 W/cm², respectively. It is revealed that with the 50 fs pulses, high harmonics are generated from neutral manganese. However, harmonics from GAR are not observed with the 50 fs pulses. The high harmonics from GAR appear for a laser with a pulse duration of 30 fs. (b) The high-harmonic spectra recorded with a few-cycle laser at an intensity of ∼4.0 × 10^14 W/cm². In these spectra, a broadband continuum is observed. The high-harmonic intensity is high at energies from 49 to 53 eV. This intensity enhancement indicates that these harmonics are generated from the GAR of neutral manganese.

can find the laser-ablated species responsible for HHG. Calculations for $\lambda = 1.8$ μm with the three-step model show that high harmonics with 50 fs pulses are generated from neutral manganese (details are given in the theoretical section).

The manganese plume contains both neutral and singly charged ions at laser-ablation conditions suitable for intense HHG [16,34]. For high harmonics from manganese, we find a difference in the cutoff when multicycle near-IR (0.8 μm; energy of ∼8 to 25 mJ) [16] and IR (1.8 μm; energy ∼1 to 5 mJ) pulses are used. With near-IR pulses, high harmonics up to 156 eV have been observed [16,26] at high laser intensities up to ∼10^15 W/cm², whereas with the

IR laser, even at similar intensities of ∼5 × 10^14 W/cm², the harmonic cutoff is observed at ∼36 eV. This difference can be explained by the fact that with a near-IR laser, high harmonics are mostly generated from ionic species [16]. Alternatively, we have observed HHG from neutral manganese showing that with an IR laser, the dominant contribution comes from neutral atoms. Therefore, with IR lasers, we could extend high-harmonic studies for neutral particles, particularly for elements containing GAR [35].

In gaseous media, high harmonics have been demonstrated for molecules of low ionization potentials (8–10 eV). However, molecules are more complex in nature than atoms since HHG process from molecules is perturbed from the rotational, vibrational, electronic excitations, and nuclear motion. Therefore, in HHG from molecules, special methods such as pump-probe schemes are required to avoid or study the additional contributions mentioned above. Furthermore, molecules are ionized at higher intensities than atoms of the same ionization potential due to the more complex orbital structure, which can suppress the tunnel-ionization amplitude [36]. Therefore, the study of neutral atoms not only will advance the laser-ablation technique for HHG but will be useful for understanding their ultrafast and attosecond dynamics.

To further extend the harmonic cutoff, the pulses were compressed to 30 fs. With these pulses, it is observed that the high-harmonic cutoff is extended from 36 to 52 eV [Fig. 2(a); blue spectra]. In these spectra, intense high harmonics at energies 49.7 and 51.1 eV are observed. The energies of these harmonics, which are the 73rd and 75th harmonics of the 1.82 μm driving field, correspond to the GAR of neutral manganese [37]. The high intensity of the harmonics around 50 eV indicates the involvement of GAR in HHG.

Since the GAR of manganese is broadband [37], the driving field was further compressed to 12 fs to see the effect of high harmonics from GAR over a broad energy range. With few-cycle pulses, an intense and broadband continuum is observed in the energy region from 49 to 53 eV [Fig. 2(b)]. Normally, high harmonics are generated from the ground state electron via the normal three-step process. In this case, the intensity of the high harmonics close to the cutoff decreases rapidly. However, it has been observed that when resonances constructively contribute to coherent HHG, the high-harmonic intensity increases dramatically [15,18,20]. In Fig. 2(b), intense high-harmonic emission of around 50 eV, which is within the bandwidth of GAR [33], confirms the involvement of GAR in HHG.

The difference in the HHG spectra with 0.8 and 1.8 μm lasers is due to the different ponderomotive energies of these fields. Namely, assuming that the photoionization of neutral Mn takes place at an intensity of 10^14 W/cm², we find that the three-step model cutoff is at a photon energy of approximately 27 and 104 eV for the 0.8 and 1.8 μm lasers,

respectively. Therefore, for the 0.8 μm field, the XUV photons near 50 eV cannot be generated by the neutral atoms, but for the 1.8 μm field, it can. The ionization probability is higher for the neutral atoms (close to unity at the peak of the laser pulse) than for the ions. Therefore, we conclude that for the 1.8 μm field, the harmonics from resonance are generated mainly by neutral atoms.

It should be noted that the GAR of manganese is different for neutral atoms and ions [38]. In neutral manganese, the GAR appears from the $3p$-$3d$ transitions only. However, in Mn$^+$, the $3p$-$4s$ channel also contributes in enhancing the PICS that appears as three additional peaks at low energies of the $3p$-$3d$ resonance peak. However, the peaks of the $3p$-$4s$ channel in HHG have not been observed. The absence of the $3p$-$4s$ peaks in spectra shown in Fig. 2(b) is another proof of HHG from neutral atoms.

One interesting aspect of studying GAR is that these resonances involve multielectron interactions [33]. The model proposed by Shiner *et al.* [8] for high-harmonic emission from xenon show that such studies might be useful to explore electron-electron correlation via Coulomb interaction between the energetic continuum electron and the inner-shell $4d$ electron. However, our observation of harmonic emission from the GAR $\sim$50 eV shows that the HHG process in manganese is different than the model proposed by Shiner *et al.* The harmonic emission exactly at 50 eV shows no Coulomb interaction between the continuum electron and the inner-shell $3p$ electron. Knowing the fact that HHG from neutral manganese involve electrons from multiple orbitals ($3p$, $3d$, and $4s$), the exact mechanism of HHG is not clear. Our results will provide roots to investigate the core process involved in HHG from the GAR and investigate their multielectron interaction. To reduce the numerical complications for the multielectron interaction, we simulate the high-harmonic spectra using the model recently proposed by Strelkov [39].

The LAP used in experiments is composed of neutral Mn and Mn$^+$, and both types of particles have ground state to autoionizing state (AIS) transitions at energies of about 50 eV. Therefore, spectra emitted by neutral Mn and Mn$^+$ were simulated. We calculate the spectra solving numerically time-dependent Schrödinger equation (TDSE) for a model atom or ion in the laser field. The numerical method is described in Ref. [40]. We use model potentials similar to the ones suggested in Refs. [20,39], which have an excited quasistable state modeling the AIS of the atom or ion. Choosing the parameters of the model potential, we reproduce the ionization energy of the generating particle, the frequency of the transition from the ground state to the AIS, and the AIS width.

The calculated spectra presented in Fig. 3 are averaged over the laser pulse carrier-envelope phase, which is not fixed in our experiments, and over the peak laser intensity. The latter averaging takes into account the spatial
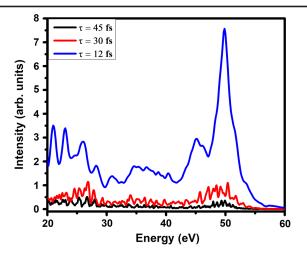

FIG. 3. Calculated high-harmonic spectra from manganese with fields of pulse durations 45 (black spectrum), 30 (red spectrum), and 12 fs (blue spectrum), and a wavelength centered at 1.82 μm. These spectra are simulated with a laser intensity of 1×10^{14} W/cm^2 as the upper limit of the intensity averaging.

distribution of the fundamental intensity in the transverse section of the laser beam (note that we do not take into account HHG phase matching in the numerical studies). The intensity averaging is very important because the low ionization potential of neutral Mn leads to HHG under relatively low laser intensities (about an order of magnitude lower than the peak laser intensity in the focus of the experimentally used beam). The relatively large volume of the target where such intensities take place provides the main contribution to the total HHG signal.

The low fundamental frequency used in experiments leads to the tunneling regime of ionization, not only for Mn$^+$ but also for neutral Mn, despite its low ionization potential. The ionization potentials of neutral Mn and Mn$^+$ differ by more than 2 times (7.4 and 15.6 eV), resulting in dramatically different HHG spectra. The cutoff position in the neutral Mn spectrum is defined not by the peak laser intensity but by the laser intensity providing complete ionization. Depending on the laser pulse duration, this intensity is about 0.3–0.5×10^{14} W/cm^2, leading to the cutoff in the HHG spectra at 35–55 eV. By contrast, Mn$^+$ is not completely ionized up to the highest laser intensity used in the experiments (5×10^{14} W/cm^2); thus, the cutoff in the HHG spectrum is at about 0.5 keV. However, our TDSE calculations show that in the spectral range under experimental consideration (up to 60 eV with the few-cycle pulse; spectra not shown) the XUV emitted by neutral atoms is much more intense than the XUV emitted by the ions. Note that, experimentally, this difference should be even more pronounced due to worse phase matching in the highly ionized medium. That is why below we present calculated results only for neutral Mn and use the intensity of 1×10^{14} W/cm^2 as the upper limit of the intensity averaging.

The TDSE solution allows one to study the ionization dynamics of Mn with laser pulses of different durations. These studies show that for a 45 fs pulse, the atoms are ionized at intensities of 0.3–0.4×10^{14} W/cm^2, corresponding to the HHG cutoff at 35–45 eV. Therefore, very few atoms survive up to higher intensities, which provide the plateau wide enough to "approach" the resonant frequency. This is why the resonant maximum is not very pronounced in the spectra. Shortening of the laser pulse leads to the surviving of a higher ratio of neutral atoms up to the intensities providing wider plateau, including the resonant frequency. Therefore, the resonant maximum appears for the 30 fs pulse and becomes highly pronounced for the 12 fs pulse.

In conclusion, we study in this Letter the application of IR fields for HHG from laser-ablated manganese. Our results show that high harmonics are observed from neutral manganese. This observation will be useful to advance high-harmonic studies from LAP from ionic species to neutral atoms with an IR field that will also reduce the laser intensity requirement of harmonic study from elements having low ionization energy. Moreover, intense and broadband high harmonics from GAR have been demonstrated in the energy region of 49–53 eV with few-cycle pulses. The harmonic emission in this energy region confirms the direct involvement of GAR in HHG. Furthermore, numerical calculations are performed to simulate the harmonic spectra and good agreement is found with the experimental results.

Our results open the possibility to generate harmonics from laser-ablated neutral particles and explore the dynamics of the GAR, such as photoionization, recombination on ultrafast timescales, and the role of multielectrons in HHG. Moreover, the intense harmonic emission from GAR will allow one to explore appropriate material [33] for broadband XUV pulse generation. It is observed that the phase emission of high harmonics from atomic resonances is different from the normal high harmonics generated from the ground state electron [41]. Further information about the phase emission will provide roots to use high harmonics from GAR directly for intense attosecond pulse production [39] or by combining them with the normal harmonics.

---

[*]Corresponding author.
ozaki@emt.inrs.ca

[1] M. Ferray, A. L'Huillier, X. F. Li, L. A. Lompre, G. Mainfray, and C. Manus, J. Phys. B **21**, L31 (1988).

[2] A. McPherson, G. Gibson, H. Jara, U. Johann, T. S. Luk, I. A. McIntyre, K. Boyer, and C. K. Rhodes, J. Opt. Soc. Am. B **4**, 595 (1987).

[3] P. B. Corkum and F. Krausz, Nat. Phys. **3**, 381 (2007).

[4] H. Wang, M. Chini, S. Chen, C.-H. Zhang, F. He, Y. Cheng, Y. Wu, U. Thumm, and Z. Chang, Phys. Rev. Lett. **105**, 143002 (2010).

[5] J. Itatani, J. Levesque, D. Zeidler, H. Niikura, H. Pépin, J. C. Kieffer, P. B. Corkum, and D. M. Villeneuve, Nature (London) **432**, 867 (2004).

[6] A. Ravasio et al., Phys. Rev. Lett. **103**, 028104 (2009).

[7] M. V. Frolov, N. L. Manakov, T. S. Sarantseva, M. Y. Emelin, M. Y. Ryabikin, and A. F. Starace, Phys. Rev. Lett. **102**, 243901 (2009).

[8] A. D. Shiner, B. E. Schmidt, C. Trallero-Herrero, H. J. Wörner, S. Patchkovskii, P. B. Corkum, J. C. Kieffer, F. Légaré, and D. M. Villeneuve, Nat. Phys. **7**, 464 (2011).

[9] P. M. Kraus, B. Mignolet, D. Baykusheva, A. Rupenyan, L. Horny, E. F. Penka, G. Grassi, O. I. Tolstikhin, J. Schneider, F. Jensen, L. B. Madsen, A. D. Bandrauk, F. Remacle, and H. J. Worner, Science **350**, 790 (2015).

[10] S. Ghimire, A. D. DiChiara, E. Sistrunk, P. Agostini, L. F. DiMauro, and D. A. Reis, Nat. Phys. **7**, 138 (2011).

[11] Y. Liang, S. Augst, S. L. Chin, Y. Beaudoin, and M. Chaker, J. Phys. B **27**, 5119 (1994).

[12] R. A. Ganeev, M. Suzuki, M. Baba, and H. Kuroda, Appl. Phys. Lett. **86**, 131116 (2005).

[13] M. A. Fareed, S. Mondal, Y. Pertot, and T. Ozaki, J. Phys. B **49**, 035604 (2016).

[14] P. B. Corkum, Phys. Rev. Lett. **71**, 1994 (1993).

[15] R. A. Ganeev, M. Suzuki, M. Baba, H. Kuroda, and T. Ozaki, Opt. Lett. **31**, 1699 (2006).

[16] R. A. Ganeev, L. B. Elouga Bom, J.-C. Kieffer, M. Suzuki, H. Kuroda, and T. Ozaki, Phys. Rev. A **76**, 023831 (2007).

[17] M. Suzuki, M. Baba, R. A. Ganeev, H. Kuroda, and T. Ozaki, Opt. Lett. **31**, 3306 (2006).

[18] J. Rothhardt, S. Hädrich, S. Demmler, M. Krebs, S. Fritzsche, J. Limpert, and A. Tünnermann, Phys. Rev. Lett. **112**, 233002 (2014).

[19] N. Rosenthal and G. Marcus, Phys. Rev. Lett. **115**, 133901 (2015).

[20] V. Strelkov, Phys. Rev. Lett. **104**, 123901 (2010).

[21] M. A. Fareed, V. V. Strelkov, N. Thire, S. Mondal, B. E. Schmidt, F. Légaré, and T. Ozaki, Nat. Commun. **8**, 16061 (2017).

[22] R. A. Ganeev, High-Order Harmonic Generation in Laser Plasma Plumes (World Scientific, Singapore, 2013).

[23] S. Klumpp, N. Gerken, K. Mertens, M. Richter, B. Sonntag, A. Sorokin, M. Braune, K. Tiedtke, P. Zimmermann, and M. Martins, New J. Phys. **19**, 043002 (2017).

[24] V. K. Dolmatov, A. S. Kheifets, P. C. Deshmukh, and S. T. Manson, Phys. Rev. A **91**, 053415 (2015).

[25] R. A. Ganeev, T. Witting, C. Hutchison, F. Frank, M. Tudorovskaya, M. Lein, W. A. Okell, A. Zaïr, J. P. Marangos, and J. W. G. Tisch, Opt. Express **20**, 25239 (2012).

[26] M. V. Frolov, N. L. Manakov, and A. F. Starace, Phys. Rev. A **82**, 023424 (2010).

[27] A. Cirri, J. Husek, S. Biswas, and L. R. Baker, J. Phys. Chem. C **121**, 15861 (2017).

[28] S. Pabst and R. Santra, Phys. Rev. Lett. **111**, 233005 (2013).

[29] D. Faccialà, S. Pabst, B. D. Bruner, A. G. Ciriolo, S. De Silvestri, M. Devetta, M. Negro, H. Soifer, S. Stagira, N. Dudovich, and C. Vozzi, Phys. Rev. Lett. **117**, 093902 (2016).

[30] J. B. West and J. Morton, At. Data Nucl. Data Tables **22**, 103 (1978).

[31] N. Thiré, S. Beaulieu, V. Cardin, A. Laramée, V. Wanie, B. E. Schmidt, and F. Légaré, Appl. Phys. Lett. **106**, 091110 (2015).

[32] V. Cardin, N. Thiré, S. Beaulieu, V. Wanie, F. Légaré, and B. E. Schmidt, Appl. Phys. Lett. **107**, 181101 (2015).

[33] M. Martins, K. Godehusen, T. Richter, P. Wernet, and P. Zimmermann, J. Phys. B **39**, R79 (2006).

[34] R. A. Ganeev, J. Phys. B **40**, R213 (2007).

[35] R. A. Ganeev, Opt. Spectrosc. **105**, 930 (2008).

[36] J. P. Marangos, J. Phys. B **49**, 132001 (2016).

[37] J. T. Costello, E. T. Kennedy, B. F. Sonntag, and C. W. Clark, Phys. Rev. A **43**, 1441 (1991).

[38] J. W. Cooper, C. W. Clark, C. L. Cromer, T. B. Lucatorto, B. F. Sonntag, E. T. Kennedy, and J. T. Costello, Phys. Rev. A **39**, 6074 (1989).

[39] V. V. Strelkov, Phys. Rev. A **94**, 063420 (2016).

[40] V.V Strelkov, A. F. Sterjantov, N. Y. Shubin, and V. T. Platonenko, J. Phys. B **39**, 577 (2006).

[41] S. Haessler, V. Strelkov, L. B. Elouga Bom, M. Khokhlova, O. Gobert, J. F. Hergott, F. Lepetit, M. Perdrix, T. Ozaki, and P. Salières, New J. Phys. **15**, 013051 (2013).